

# Enhancement of Nuclear Spin-Lattice Relaxation Rate and Spin Susceptibility due to Valence Fluctuations -Origin of Anomalously Enhanced Wilson Ratio in Ce and Yb Systems-

Shinji Watanabe<sup>1</sup> and Kazumasa Miyake<sup>2</sup>

*Department of Applied Physics, University of Tokyo,  
Hongo 7-3-1, Bunkyo-ku, Tokyo, 113-8656, Japan<sup>1</sup>*

*Division of Materials Physics, Department of Materials Engineering Science,  
Graduate School of Engineering Science, Osaka University, Toyonaka, Osaka 560-8531, Japan<sup>2</sup>*

(Dated: November 24, 2008)

We show theoretically that the nuclear spin-lattice relaxation rate  $(T_1T)^{-1}$  and the spin susceptibility  $\chi_s(T)$  exhibit divergent behaviors toward zero temperature at the quantum critical point (QCP) of the first-order valence transition. Remarkable enhancement in  $(T_1T)^{-1}$  and  $\chi_s(T)$  is induced by valence fluctuations even at the valence-crossover temperature far away from the QCP. This mechanism well explains peculiar behaviors observed recently in  $\text{YbAuCu}_4$  and also gives a systematic explanation for  $\text{YbXCu}_4$  for  $X=\text{In, Au, Ag, Tl, and Pd}$  from the viewpoint of the closeness to the QCP. This also explains anomalously enhanced Wilson ratio observed in the paramagnetic Ce and Yb based compounds. This offers a new concept that spin fluctuations are induced via relative charge fluctuations, which can be generally applied to the systems with valence instabilities.

PACS numbers: 71.27.+a, 75.20.Hr, 71.10.-w, 71.20.Eh

Quantum critical phenomena in strongly-correlated electron systems have been discussed extensively in the context of magnetic phase transitions [1, 2, 3]. Recently, instabilities in charge sectors have attracted much attention, since underlying influence of valence instability is suggested by variety of materials [4, 5, 6, 7]: Importance of critical valence fluctuations has been argued as a possible origin of anomalies such as  $T$ -linear resistivity, enhanced residual resistivity and superconductivity for the materials with valence-fluctuating ions such as Ce and Yb.

Valence transition is isostructural transition as known as  $\gamma$ - $\alpha$  transition in Ce metal [8] and also in  $\text{YbInCu}_4$  [9] characterized by a jump of the valence of the Ce and Yb ion. In  $\text{YbInCu}_4$  the first-order valence transition at  $T = 42$  K takes place with the valence of Yb being +2.97 (+2.84) in the high (low)-temperature phase [10]. Interestingly, anomalous behaviors in the  $\text{YbXCu}_4$  have been revealed by systematic measurements: A remarkable enhancement in the nuclear spin-lattice relaxation rate  $(T_1T)^{-1}$  has been discovered recently for  $X=\text{Au}$  [11, 12]. A mysterious behavior of this material has been recognized in the spin susceptibility, which increases enormously toward zero temperature [13] in spite of the antiferromagnetically-ordered ground state with  $T_N \sim 0.8$  K [14]. By applying the magnetic field  $T_N$  is suppressed to 0 K at  $H_c \sim 1.3$  T and a remarkable point is that by further applying  $H$  the enhancement of  $(T_1T)^{-1}$  emerges at finite temperature,  $T = T_v(H)$  [11, 12]. Since these anomalies appear even far away from  $H_c$ , i.e., in the regime where the magnetic order is completely destroyed, this is not due to the magnetic fluctuations.

Furthermore, it has been discovered that the  $^{63}\text{Cu}$  NQR frequency  $\nu_Q$  shows a sharp drop at  $T_v$  when  $T$  decreases [12]. Since  $\nu_Q$  measures the charge distribution of the Yb and surrounding ions, the change of  $\nu_Q$

indicates that the Yb valence changes at  $T_v$  sharply. A peak structure in the spin susceptibility  $\chi_s(T)$  at  $T_v$  has been also detected for  $X=\text{Ag}$  [13] and  $\text{Tl}$  [13], and enhancement in  $(T_1T)^{-1}$  has been also found at  $T_v$  for  $X=\text{Ag}$  [16] and  $X=\text{Pd}$  [17] recently. These observations suggest that this behavior is not specific to a special material, but is rather universal. Since valence fluctuations are ascribed to the relative charge fluctuations between  $f$  and conduction electrons, these observations challenge the conventional concept that the nuclear spin-lattice relaxation rate and the spin susceptibility reflect magnetic fluctuations in the paramagnetic-metal phase.

In this Letter, we resolve this puzzle by showing that valence fluctuations indeed induce spin fluctuations. We show that  $(T_1T)^{-1}$  as well as  $\chi_s(T)$  shows divergence toward zero temperature at the quantum critical point (QCP) of the valence transition. Even in the valence-crossover region at finite temperatures away from the QCP,  $(T_1T)^{-1}$  and  $\chi_s(T)$  are shown to be enhanced. This mechanism gives a systematic explanation for peculiar behaviors observed in  $\text{YbXCu}_4$  for  $X=\text{In, Au, Ag, Tl and Pd}$ , and also accounts for anomalously enhanced Wilson ratio observed in several Yb and Ce materials located near the QCP of the valence transition. This result offers a new concept that spin fluctuations are induced via relative charge fluctuations, which can be generally applied to the systems with valence instabilities.

Let us start our analysis by introducing a minimal model which describes the essential part of the Yb and Ce systems in the standard notation [18, 19]:

$$H = H_c + H_f + H_{\text{hyb}} + H_{U_{\text{fc}}}, \quad (1)$$

where  $H_c = \sum_{\mathbf{k}\sigma} \varepsilon_{\mathbf{k}} c_{\mathbf{k}\sigma}^\dagger c_{\mathbf{k}\sigma}$ ,  $H_f = \varepsilon_f \sum_{i\sigma} n_{i\sigma}^f + U_{\text{ff}} \sum_{i=1}^N n_{i\uparrow}^f n_{i\downarrow}^f$ ,  $H_{\text{hyb}} = \sum_{\mathbf{k}\sigma} V_{\mathbf{k}} \left( f_{\mathbf{k}\sigma}^\dagger c_{\mathbf{k}\sigma} + c_{\mathbf{k}\sigma}^\dagger f_{\mathbf{k}\sigma} \right)$  and  $H_{U_{\text{fc}}} = U_{\text{fc}} \sum_{i=1}^N n_i^f n_i^c$ . The  $U_{\text{fc}}$  term is the Coulomb

repulsion between  $f$  and conduction electrons, which is considered to play an important role in the valence transition: In the case of Ce metal which exhibits the  $\gamma$ - $\alpha$  transition, the 4 $f$ - and 5 $d$ -electron bands are located at the Fermi level [20]. Since both the orbitals are located on the same Ce site, this term cannot be neglected. For YbInCu<sub>4</sub>, the considerable magnitude of the In 5 $p$  and Yb 4 $f$  hybridization was pointed out by the band-structure calculation [21] and recent high-resolution photoemission spectra has detected a remarkable increase of the  $p$ - $f$  hybridization at the first-order valence transition [22]. These results suggest importance of  $V_{\mathbf{k}}$  and  $U_{\text{fc}}$ . Actually, the reason why the critical-end temperature is so high as much as 600 K in Ce metal in contrast to that in YbInCu<sub>4</sub> can be understood in terms of  $U_{\text{fc}}$ : In YbInCu<sub>4</sub>,  $U_{\text{fc}}$  is the intersite interaction, which should be smaller than that of Ce metal. This view also gives an explanation for the reason why most of Ce and Yb compounds only shows the valence crossover. Namely, most of the compounds seems to have a moderate value of  $U_{\text{fc}}$  due to its intersite origin, which is smaller than the critical value to cause a jump of the valence. However, even in the valence-crossover regime, underlying influence of the valence instability causes intriguing phenomena as shown below. It is noted that importance of  $U_{\text{fc}}$  has been discussed by several authors for YbInCu<sub>4</sub> [23, 24].

In this model (1) the first-order transition between the larger  $\langle n_f \rangle$  and the smaller  $\langle n_f \rangle$  is caused by  $U_{\text{fc}}$ , since the large  $U_{\text{fc}}$  forces electrons to pour into either the  $f$  level or the conduction band [7, 25]. Figure 1(a) shows the ground-state phase diagram in the  $\varepsilon_f$ - $U_{\text{fc}}$  plane determined by the density-matrix renormalization group (DMRG) for  $\varepsilon_{\mathbf{k}} = -2 \cos(k)$ ,  $V = V_{\mathbf{k}} = 0.1$  and  $U = 100$  at filling  $\sum_{i=1}^N \langle n_i^f + n_i^c \rangle / (2N) = 7/8$  [7]. We note that essentially the same phase diagram has been obtained in the infinite dimensional system [26]. The first-order-transition line (brown line) separates the paramagnetic-metal phase, namely, the larger  $\langle n_f \rangle$  phase in the smaller  $\varepsilon_f$  and  $U_{\text{fc}}$  regime, and the smaller  $\langle n_f \rangle$  phase in the larger  $\varepsilon_f$  and  $U_{\text{fc}}$  regime. As  $U_{\text{fc}}$  decreases the jump in  $n_f$  at the first-order transition decreases and terminates at the QCP, at which the valence fluctuation diverges.

The valence fluctuation is measured by the dynamical valence susceptibility defined by  $\chi^{\text{ff}}(\mathbf{q}, i\omega_n) \equiv \int_0^\beta d\tau \langle T_\tau n^f(\mathbf{q}, \tau) n^f(-\mathbf{q}, 0) \rangle e^{i\omega_n \tau}$  with  $\omega_n = 2n\pi T$  ( $n = 0, \pm 1, \pm 2, \dots$ ). The most dominant part of  $\chi^{\text{ff}}$  near the QCP is expressed by the four-point vertex function  $\Gamma$  in Fig. 2(a), which satisfies the integral equation shown in Fig. 2(b). Here, the solid line and dashed line represent quasiparticle parts of Green functions near the Fermi level  $G_{\sigma}^{\text{ff}}(\mathbf{q}, i\varepsilon_n) \sim 1/(i\varepsilon_n - E_{\mathbf{q}\sigma}^*)$ ,  $G_{\sigma}^{\text{cc}}(\mathbf{q}, i\varepsilon_n) \sim 1/(i\varepsilon_n - E_{\mathbf{q}\sigma}^*)$ , respectively, where  $\varepsilon_n = (2n+1)\pi T$  and the origin of the energy is set as  $\mu \equiv 0$ . Here,  $E_{\mathbf{q}\sigma}^*$  satisfies  $(z - \varepsilon_f - \Sigma_{\mathbf{q}\sigma}^{\text{ff}}(z))(z - \varepsilon_{\mathbf{q}}) - |\tilde{V}_{\mathbf{q}\sigma}(z)|^2 = 0$  ( $z = E_{\mathbf{q}\sigma}^*$ ), where  $\tilde{V}_{\mathbf{q}\sigma}(z) \equiv V_{\mathbf{q}} + \Sigma_{\mathbf{q}\sigma}^{\text{fc}}(z)$  with  $\Sigma_{\mathbf{q}\sigma}^{\text{ff}}$  and  $\Sigma_{\mathbf{q}\sigma}^{\text{fc}}$  being the self energies due to  $U_{\text{ff}}$  and  $U_{\text{fc}}$ , respectively. The effect of the renormalization ampli-

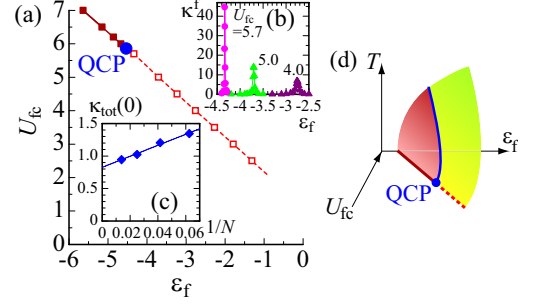


FIG. 1: (Color) (a) Ground-state phase diagram determined by the DMRG for  $\varepsilon_{\mathbf{k}} = -2 \cos(k)$ ,  $V = V_{\mathbf{k}} = 0.1$  and  $U = 100$  at filling  $\sum_{i=1}^N \langle n_i^f + n_i^c \rangle / (2N) = 7/8$  [7]. (b) Valence susceptibility has a peak on the dashed line in (a). (c) System-size dependence of the total-charge compressibility at the QCP ( $\varepsilon_f, U_{\text{fc}} = (-4.5206, 5.8460)$ ). (d) Schematic phase diagram in the  $\varepsilon_f$ - $U_{\text{fc}}$ - $T$  space for a certain  $V_{\mathbf{k}}$  and  $U_{\text{ff}}(> U_{\text{fc}})$ . The first-order valence transition surface (brown surface) with the critical end line (blue line) touched on  $T = 0$  at the QCP continues to the valence-crossover surface (light-green surface). The valence-crossover surface at which  $\kappa^f(T)$  has a maximum is denoted as  $T_v$  (see text).

tude defined by  $a_{\mathbf{q}\sigma}^{\text{ff}} \equiv [1 - \partial \Sigma_{\mathbf{q}\sigma}^{\text{ff}}(\varepsilon) / \partial \varepsilon + |\tilde{V}_{\mathbf{q}\sigma}(\varepsilon)|^2 / (\varepsilon - \varepsilon_{\mathbf{q}})^2 - 2 \text{Re}[\tilde{V}_{\mathbf{q}\sigma}^*(\varepsilon) \partial \Sigma_{\mathbf{q}\sigma}^{\text{fc}}(\varepsilon) / \partial \varepsilon] / (\varepsilon - \varepsilon_{\mathbf{q}})]^{-1}|_{\varepsilon=0}$  and  $a_{\mathbf{q}\sigma}^{\text{cc}} \equiv a_{\mathbf{q}\sigma}^{\text{ff}} |\tilde{V}_{\mathbf{q}\sigma}(0)|^2 / \varepsilon_{\mathbf{q}}^2$  is absorbed in the definition of vertex functions, internal and external [27]. The vertex  $\bar{\Gamma}$  consists of the interactions via  $U_{\text{fc}}$  with vertex parts including  $U_{\text{ff}}$ , whose contributions are represented by the double wigly line as  $\tilde{U}_{\text{fc}}$  in Fig. 2(c) and all the other contributions such as entangled  $U_{\text{fc}}$  and  $U_{\text{ff}}$  shown as  $\bar{\Gamma}_{\text{ff}}^{\sigma\sigma'}$  in Fig. 2(d). Here,  $\bar{\Gamma} = \hat{a} \tilde{U}_{\text{fc}} \hat{I} \hat{\chi}^{\parallel}$ , where  $\hat{a}$  and  $\hat{\chi}^{\parallel}$  are the  $2 \times 2$  matrices with elements  $[\hat{a}]_{\sigma\sigma'} \equiv a_{\sigma\sigma'}^{\text{ff}} a_{\sigma\sigma'}^{\text{cc}}$  and  $[\hat{\chi}^{\parallel}]_{\sigma\sigma'} = \bar{\chi}_{\sigma\sigma'}$ , defined as Fig 2(d), respectively.  $\hat{I}$  is the unit matrix. Then, we have  $\chi^{\text{ff}} \propto \text{Tr}[\hat{\chi}^{\parallel} (\hat{I} - \tilde{U}_{\text{fc}} \hat{\chi}^{\parallel})^{-1}]$ . By using the relation  $\bar{\chi}_{\text{charge}} \equiv \bar{\chi}_{\uparrow\uparrow} + \bar{\chi}_{\uparrow\downarrow}$  and  $\bar{\chi}_{\text{spin}}^{\parallel} \equiv \bar{\chi}_{\uparrow\uparrow} - \bar{\chi}_{\uparrow\downarrow}$  and noting the fact that  $\bar{\chi}_{\text{charge}} \ll \bar{\chi}_{\text{spin}}^{\parallel}$  holds for typical heavy-electron systems [28], we have  $\chi^{\text{ff}} \propto \bar{\chi}_{\text{spin}}^{\parallel} / (1 - \tilde{U}_{\text{fc}} \bar{\chi}_{\text{spin}}^{\parallel})$ .

Figure 1(d) illustrates the schematic phase diagram in the  $T$ - $\varepsilon_f$ - $U_{\text{fc}}$  space. At the critical end line of the first-order transition illustrated by the blue line in Fig. 1(d) where the denominator of  $\chi^{\text{ff}}$  equals zero,  $1 - \tilde{U}_{\text{fc}} \bar{\chi}_{\text{spin}}^{\parallel}(\mathbf{0}, 0) = 0$ , the valence susceptibility  $\kappa^f \equiv \chi^{\text{ff}}(\mathbf{0}, 0) = -\partial \langle n^f \rangle / \partial \varepsilon_f$  diverges. Note here that  $\kappa^f$  shows not only divergence at the critical-end line, but also has a maximum at the valence-crossover surface ( $\kappa^f$  has a peak in Fig. 1(b) on the dashed line in Fig. 1(a)), which is illustrated as the surface extended from the first-order one in Fig. 1(d) [7, 25]. This implies that even if the system is away from the critical end line, the valence fluctuation is enhanced at the crossover surface  $T_v$  in the parameter space of  $T$  and pressure and/or chemical doping. Furthermore, it has been revealed recently that even

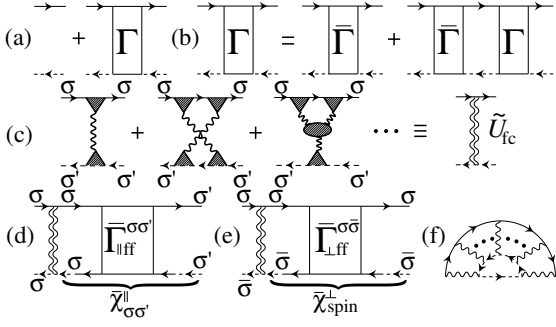


FIG. 2: (a) The most dominant part near the QCP of  $\chi^{\text{ff}}$  and  $\chi_{+-}^{\text{ff}}$  with four-point vertex  $\tilde{\Gamma}$  and (b) its integral equation. (c) Vertex parts including  $U_{\text{ff}}$  (hatched area) connected by  $U_{\text{fc}}$  (wiggly line). All contribution of this type is represented by the double wiggly line as  $\tilde{U}_{\text{fc}}$ . (d)  $\tilde{\Gamma}$  for  $\chi^{\text{ff}}$  and (e) for  $\chi_{+-}^{\text{ff}}$ .  $\bar{\sigma}$  is antiparallel spin to  $\sigma$ .  $\tilde{\Gamma}_{\text{ff}}$  contains all contributions other than the diagrams expressed in (c). (f) RPA-type self energy for  $U_{\text{fc}}$ . The solid line and dashed line represent  $G_{\sigma}^{\text{ff}}$  and  $G_{\sigma}^{\text{cc}}$ , respectively.

in the valence-crossover regime, the critical point is induced by applying the magnetic field [29]. This explains the role of the magnetic field in the  $T$ - $H$  phase diagram of YbAuCu<sub>4</sub> [11] and YbPdCu<sub>4</sub> [17]. Namely, the magnetic field not only destroys the magnetic order, but also plays a role to make the valence-crossover temperature  $T_{\text{v}}$  finite. This is consistent with the experimental fact that  $T_{\text{v}}(H)$  emerges under  $H$  even much larger than  $H_{\text{c}}$  in the  $T$ - $H$  plane, at which  $\nu_{\text{Q}}$  shows a sharp change.

Now let us focus on the nuclear spin-lattice relaxation rate defined by  $\frac{1}{T_1} = \frac{\gamma_{\text{f}}^2 k_{\text{B}} T}{g_{\text{f}}^2 \mu_{\text{B}}^2} \sum_{\mathbf{q}} |\tilde{A}_{\mathbf{q}}|^2 \frac{\text{Im} \chi_{+-}^{\text{ff}}(\mathbf{q}, i\omega_0)}{\omega_0}$ , where  $\gamma_{\text{f}}$  is the gyromagnetic ratio of nuclear spin,  $g_{\text{f}}$  is a Lande's  $g$  factor for  $\text{f}$  electrons and  $\tilde{A}_{\mathbf{q}}$  is the hyperfine-coupling constant. The dynamical  $\text{f}$ -spin susceptibility is defined by  $\chi_{+-}^{\text{ff}}(\mathbf{q}, i\omega_n) \equiv \int_0^{\beta} d\tau \langle T_{\tau} S_{+}^{\text{f}}(\mathbf{q}, \tau) S_{-}^{\text{f}}(-\mathbf{q}, 0) \rangle e^{i\omega_n \tau}$ . We note here that  $\chi_{+-}^{\text{ff}}$  has essentially the same structure as  $\chi^{\text{ff}}$ , whose most dominant terms near the QCP is expressed in Figs. 2(a) and (b). The vertex  $\tilde{\Gamma}$  in Fig. 2(b) is given by  $\tilde{\Gamma} = a_{\sigma}^{\text{ff}} a_{\bar{\sigma}}^{\text{cc}} \tilde{U}_{\text{fc}} \tilde{\chi}_{\text{spin}}^{\perp}$  as shown in Figs. 2(e) and (c). Then, we have  $\chi_{+-}^{\text{ff}} \propto \tilde{\chi}_{\text{spin}}^{\perp} / (1 - \tilde{U}_{\text{fc}} \tilde{\chi}_{\text{spin}}^{\perp})$ . Since SU(2) symmetry of the system ensures  $\tilde{\chi}_{\text{spin}}^{\perp} = \tilde{\chi}_{\text{spin}}^{\parallel}$ , it turns out that  $\chi_{+-}^{\text{ff}}$  has the same form as  $\chi^{\text{ff}}$ . Hence, at the critical-end line as well as the QCP of the valence transition (blue line in Fig 1(d)),  $1 - \tilde{U}_{\text{fc}} \tilde{\chi}_{\text{spin}}^{\perp}(\mathbf{0}, 0) = 0$  holds, which makes  $\chi_{+-}^{\text{ff}}(\mathbf{0}, 0)$  diverge [30]. Since the spectral weight of  $\text{f}$  electrons is dominated by the incoherent part around  $\varepsilon \sim \varepsilon_{\text{f}}$ , the coherent part responsible for quasiparticles amounts to a tiny contribution in the order of  $a_{\mathbf{k}_{\text{F}}\sigma}^{\text{ff}} \sim m_{\text{band}}/m^{*} \ll 1$ . Then, the  $\mathbf{q}$  dependence of  $\tilde{\chi}_{\text{spin}}^{\perp}(\mathbf{q}, i\omega_0)$  is estimated as  $\tilde{\chi}_{\text{spin}}^{\perp}(\mathbf{q}, i\omega_0) \sim \tilde{\chi}_{\text{spin}}^{\perp}(\mathbf{0}, 0) [1 + \bar{A}q^2 - i\bar{C}\omega_0/q]$  with  $\bar{A}$  in the order of  $\mathcal{O}(V_{\mathbf{k}_{\text{F}}}/|\varepsilon_{\text{f}}|)^2 \lesssim 10^{-1}$  for typical heavy-electron systems

with the spherical Fermi surface with  $q = |\mathbf{q}|$  [4]. Then, the most singular term is evaluated to show the  $(T_1 T)^{-1} \sim q^{d-5}$  divergence for  $q \rightarrow 0$  in the  $d$ -dimensional system. This result is in sharp contrast to the single-orbital system where charge instability does not occur simultaneously with the spin instability.

The uniform spin susceptibility is defined by  $\chi_{\text{s}}(T) \equiv \chi_{\text{s}}^{\text{f}}(T) + \chi_{\text{s}}^{\text{c}}(T)$  with  $\chi_{\text{s}}^{\text{a}} = \partial m^{\text{a}} / \partial H|_{H=0}$  and  $m^{\text{a}} \equiv \sum_i \langle S_i^{\text{a}z} \rangle / N$ , when the magnetic field is applied to (1) as  $-g_{\text{f}} \mu_{\text{B}} H \sum_i S_i^{\text{f}z} - g_{\text{c}} \mu_{\text{B}} H \sum_i S_i^{\text{c}z}$ . By using the dynamical spin susceptibility  $\chi_{+-}^{\text{ab}}(\mathbf{q}, i\omega_n) \equiv \int_0^{\beta} d\tau \langle T_{\tau} S_{+}^{\text{a}}(\mathbf{q}, \tau) S_{-}^{\text{b}}(-\mathbf{q}, 0) \rangle e^{i\omega_n \tau}$ ,  $\chi_{\text{s}}(T)$  is expressed as  $\chi_{\text{s}}(T) = \frac{3}{2} \mu_{\text{B}}^2 [g_{\text{f}}^2 \chi_{+-}^{\text{ff}} + g_{\text{f}} g_{\text{c}} \chi_{+-}^{\text{fc}} + g_{\text{c}} g_{\text{f}} \chi_{+-}^{\text{cf}} + g_{\text{c}}^2 \chi_{+-}^{\text{cc}}]$ , where  $\mathbf{q}$  and  $\omega_n$  are set to be zero in the right hand side (r.h.s.). In heavy-electron systems, the uniform spin susceptibility is dominated by the  $\text{f}$ -electron part as  $\chi_{\text{s}}^{\text{f}}(0) \gg \chi_{\text{s}}^{\text{c}}(0)$  [28]. Then,  $g_{\text{f}}^2 \chi_{+-}^{\text{ff}} + g_{\text{f}} g_{\text{c}} \chi_{+-}^{\text{fc}} \gg g_{\text{c}} g_{\text{f}} \chi_{+-}^{\text{cf}} + g_{\text{c}}^2 \chi_{+-}^{\text{cc}}$  holds. Since  $\chi_{+-}^{\text{fc}} = \chi_{+-}^{\text{cf}}$ , we have  $\chi_{\text{s}}(T) \sim (3/2) \mu_{\text{B}}^2 g_{\text{f}}^2 \chi_{+-}^{\text{ff}}$ . Hence, at the QCP,  $\chi_{\text{s}}(0)$  shows  $\omega_{\text{v}}^{-1}$  divergence with  $\omega_{\text{v}} \equiv 1 - \tilde{U}_{\text{fc}} \tilde{\chi}_{\text{spin}}^{\parallel}(\mathbf{0}, 0)$ .

We note here that quite different behavior appears in the charge sector: Our DMRG calculation applied to the Hamiltonian (1) shows that even at the QCP of the valence transition where  $\kappa^{\text{f}}$  diverges, the total charge compressibility  $\kappa_{\text{tot}} \equiv \partial \langle n^{\text{f}} \rangle / \partial \mu + \partial \langle n^{\text{c}} \rangle / \partial \mu$  does not diverge (see Fig. 1(c)). Namely, the r.h.s. of  $\kappa_{\text{tot}}(0) = \chi^{\text{ff}} + \chi^{\text{fc}} + \chi^{\text{cf}} + \chi^{\text{cc}}$  are cancelled each other to give a finite value in spite that  $\chi^{\text{ff}}$  diverges. Here,  $\mathbf{q}$  and  $\omega_n$  are set to be zero in  $\chi^{\text{ab}}(\mathbf{q}, i\omega_n) \equiv \int_0^{\beta} d\tau \langle T_{\tau} n^{\text{a}}(\mathbf{q}, \tau) n^{\text{b}}(-\mathbf{q}, 0) \rangle e^{i\omega_n \tau}$ . This is in sharp contrast to the mean-field result, where the first-order valence transition is accompanied by the phase separation. Namely, diverging relative charge fluctuation (i.e., valence fluctuation) also induces the instability of the total charge in the mean-field framework. However, our finding shows that quantum fluctuations and electron correlations can make the total charge stable even though the relative charge unstable. This is ascribed to the fact that the order parameter of the valence transition,  $n^{\text{f}} = \sum_{i=1}^N n_i^{\text{f}}$  is not the conserving quantity, i.e.,  $[n^{\text{f}}, H]_{-} \neq 0$  [7]. This result indicates that the first-order valence transition is not accompanied by the phase separation at least in electronic origin. We point out that the  $g$  factors in  $\chi_{\text{s}}(T)$ , which usually differs between  $\text{f}$  and conduction electrons, i.e.,  $g_{\text{f}} \neq g_{\text{c}}$  prevent from the cancellation among  $\chi_{+-}^{\text{ab}}$  as occurred in the r.h.s. of  $\kappa_{\text{tot}}(0)$ , and hence the divergent behavior can emerge in  $\chi_{\text{s}}(0)$  in contrast to  $\kappa_{\text{tot}}(0)$ .

The enhanced  $\chi_{\text{s}}(T)$  toward low temperature has been observed in YbAuCu<sub>4</sub> [13]. The NQR and susceptibility measurements suggest that YbAuCu<sub>4</sub> is located near the QCP of the valence transition at  $H = 0$  [12], although the antiferromagnetic order masks the ground state with  $T_{\text{N}} = 0.8$  K. Namely, the valence-crossover temperature  $T_{\text{v}}$  is suppressed to be close to  $T = 0$  K so that  $\chi_{\text{s}}(T)$  is interpreted to be enhanced toward low temperature by the critical valence fluctuations. On the other hand, in YbAgCu<sub>4</sub> where no magnetic transition has been ob-

served at ambient pressure at  $H = 0$ , the lattice constant changes around  $T_v = 40$  K, suggesting the valence crossover [15]. A remarkable point is that  $\chi_s(T)$  has a peak at  $T_v$  [13], whose maximum value is one order of magnitude smaller than that of YbAuCu<sub>4</sub>. This is again consistent with our theory, since at finite  $T_v$ , i.e., at the valence-crossover point  $\chi_s(T_v)$  is enhanced but does not diverge, while in the case of  $T_v = 0$ , i.e., at the QCP  $\chi_s(0)$  diverges (see Fig. 1(b) and Fig. 1(d)). We note that a recent  $(T_1T)^{-1}$  measurement has also detected a broad peak around  $T_v$  in YbAgCu<sub>4</sub> [16]. It is noted that the maximum in  $\chi_s(T)$  has been also observed at  $T_v$  for X=Tl [13]. Hence, as X moves as Au, Ag to Tl,  $T_v$  increases, i.e., the distance from the QCP becomes long, which makes the peak value of the spin susceptibility  $\chi_s(T_v)$  small. Then, our theory explains these systematic observations quite consistently.

Finally, we argue the Wilson ratio near the QCP. The self energy for f electrons is given by  $\tilde{\Sigma}_\sigma^{\text{ff}}(\mathbf{p}, i\varepsilon_n) = \frac{T}{N} \sum_{\mathbf{q}, m} \frac{2U_{\text{fc}}G_\sigma^{\text{cc}}(\mathbf{p}-\mathbf{q}, i\varepsilon_n - i\omega_m)}{1 - U_{\text{fc}}\tilde{\chi}_\sigma^{\text{fc}}(\mathbf{q}, i\omega_m)}$  within the RPA as illustrated in Fig. 2(f). Here,  $\tilde{\chi}_\sigma^{\text{fc}}(\mathbf{q}, i\omega_m) \equiv -\frac{T}{N} \sum_{\mathbf{k}, n} G_\sigma^{\text{ff}}(\mathbf{k}, i\varepsilon_n) G_\sigma^{\text{cc}}(\mathbf{k} + \mathbf{q}, i\varepsilon_n + i\omega_m)$  where  $G_\sigma^{\text{ff}}(\mathbf{k}, i\varepsilon_n) = \bar{a}_{\mathbf{k}\sigma}^{\text{ff}}/(i\varepsilon_n - E_{\mathbf{k}\sigma}^*) + G_{\text{inc}}^{\text{ff}}$  and  $G_\sigma^{\text{cc}}(\mathbf{k}, i\varepsilon_n) = \bar{a}_{\mathbf{k}\sigma}^{\text{cc}}/(i\varepsilon_n - E_{\mathbf{k}\sigma}^*) + G_{\text{inc}}^{\text{cc}}$  with  $U_{\text{fc}}$  set to be zero in the previous definition of  $E_{\mathbf{q}\sigma}^*$ . Here,  $\bar{a}_{\mathbf{k}\sigma}^{\text{ff}} \equiv [1 - \partial \Sigma_{\mathbf{k}\sigma}^{\text{ff}}(\varepsilon)/\partial \varepsilon|_{\varepsilon=0} + V_{\mathbf{k}}^2/\varepsilon_{\mathbf{k}}^2]^{-1}$  and  $\bar{a}_{\mathbf{k}\sigma}^{\text{cc}} \equiv \bar{a}_{\mathbf{k}\sigma}^{\text{ff}} V_{\mathbf{k}}^2/\varepsilon_{\mathbf{k}}^2$ , and  $G_{\text{inc}}^{\text{ff}}$  and  $G_{\text{inc}}^{\text{cc}}$  denote the incoherent parts. Near the QCP small  $\mathbf{q}$  and  $\omega$  components are important and the denominator of  $\tilde{\Sigma}_\sigma^{\text{ff}}$  is expanded as  $1 - U_{\text{fc}}\tilde{\chi}_\sigma^{\text{fc}}(\mathbf{q}, \omega + i\delta) \sim \bar{\omega}_v + Aq^2 - iC\omega/q$  with  $\bar{\omega}_v \equiv 1 - U_{\text{fc}}\tilde{\chi}_\sigma^{\text{fc}}(\mathbf{0}, 0)$  [4]. Then, we evaluate  $m^*/m_{\text{band}} = 1 - \partial \text{Re}\tilde{\Sigma}_\sigma^{\text{ff}}(\mathbf{p}_F, \varepsilon)/\partial \varepsilon|_{\varepsilon=0} = 1 - (\bar{a}_{\mathbf{p}_F\sigma}^{\text{cc}} U_{\text{fc}}/(4\pi^2 v_F A)) \ln[\bar{\omega}_v/(\bar{\omega}_v + Aq_c^2)]$  to the leading order of  $\bar{a}_{\mathbf{p}_F\sigma}^{\text{cc}} \sim \bar{a}_{\mathbf{p}_F\sigma}^{\text{ff}}$ , where  $v_F$  is the Fermi velocity and  $q_c$  is a cut-off. Namely, the Sommerfeld constant  $\gamma_e$  shows a log divergence at the QCP. Since  $\chi_s(0)$  shows a  $\bar{\omega}_v^{-1}$  divergence, the Wilson ratio  $R_W = 4\pi^2 k_B^2 \chi_s/(3(g\mu_B)^2 \gamma_e)$  diverges at the QCP of the valence transition ( $\bar{\omega}_v \rightarrow 0$ ).

Although the Gaussian fixed point of the QCP of the valence transition ensures the validity of the RPA description [4], more qualitatively  $\bar{\omega}_v$  should be determined self-consistently as done in the SCR theory for spin fluctuations [1]. This kind of analysis can be executed for valence fluctuations starting from the valence susceptibility  $\chi^{\text{ff}}(\mathbf{q}, \omega)^{-1} \sim \bar{\omega}_v + Aq^2 - iC_q\omega$ , expanded near  $(\mathbf{q}, \omega) = (\mathbf{0}, 0)$ . Here,  $C_q$  is given, in the  $T \rightarrow 0$  limit, by the form  $C/\max\{q, l^{-1}\}$  with  $l$  being the mean free path of the impurity scattering [32]. Then, in the realistic situation, the dynamical exponent  $z_d = 3$  is expected to be observed at low  $T$ , except in the very vicinity of  $T = 0$  K where impurity scattering is dominant and hence the system is described by  $z_d = 2$  [33]. Since in the three dimension with  $z_d = 3$  the susceptibility and Sommerfeld constant behave as  $\chi_s(T) \sim T^{-4/3}$  and  $\gamma_e \sim -\ln T$ , respectively, in case that incoherent part of f electrons gives minor contributions to the criticality, the Wilson ratio diverges in this case, too. Namely, our results based on the RPA are considered to be qualitatively correct and more quantitative arguments for comparison with experiments will be reported in the separated paper [34].

We note that  $\chi_s(0)$  and  $\gamma_e$  extrapolated to  $T \rightarrow 0$  K from the  $T > T_N = 0.8$  K data in YbAuCu<sub>4</sub> shows  $R_W \sim 4.5$  [13], which exceeds  $R_W = 2$ . Enhanced Wilson ratio  $R_W \sim 3$  has been also observed in Ce<sub>0.9-x</sub>La<sub>x</sub>Th<sub>0.1</sub> with  $x = 0.1$  [31] where the  $\gamma$ - $\alpha$ -transition temperature is suppressed closely to zero temperature. These materials are located near the QCP of the valence transition and hence our theory gives an explanation for these enhancements. Enhanced  $R_W$  has been also observed in other paramagnetic materials such as YbRh<sub>2</sub>(Si<sub>0.95</sub>Ge<sub>0.05</sub>)<sub>2</sub> [35], YbIr<sub>2</sub>Si<sub>2</sub> [36] and  $\beta$ -YbAlB<sub>4</sub> [37], which also suggests underlying influence of valence fluctuations.

We stress that our results can be generally applied to the systems with valence instabilities. Experimental examination of our predictions is highly desired.

The authors thank S. Wada and S. Nakatsuji for showing us their experimental data prior to publication.

- 
- [1] T. Moriya, *Spin Fluctuations in Itinerant Electron Magnetism* (Springer-Verlag, Berlin, 1985).
  - [2] J. A. Hertz, Phys. Rev. B **14**, 1165 (1976).
  - [3] A. J. Millis, Phys. Rev. B **48**, 7183 (1993).
  - [4] K. Miyake, J. Phys.: Condens. Matter **19**, 125201 (2007).
  - [5] H. Q. Yuan *et al.*, Science **302**, 2104 (2003).
  - [6] A. T. Holmes *et al.*, Phys. Rev. B **69**, 024508 (2004).
  - [7] S. Watanabe *et al.*, J. Phys. Soc. Jpn. **75**, 043710 (2006).
  - [8] K. A. Gschneidner and L. Eyring, *Handbook on the Physics and Chemistry of Rare Earths* (North-Holland, Amsterdam, 1978).
  - [9] I. Felner and I. Nowik, Phys. Rev. B **33**, 617 (1986).
  - [10] A. L. Cornelius *et al.*, Phys. Rev. B **56**, 7993 (1997); C. Dallera *et al.*, Phys. Rev. Lett. **88**, 196403 (2002); Y. H. Matsuda *et al.*, J. Phys. Soc. Jpn. **76**, 034702 (2007).
  - [11] A. Yamamoto *et al.*, J. Phys. Soc. Jpn. **76**, 063709 (2007).
  - [12] S. Wada *et al.*, J. Phys.: Condens. Matter **20**, 175201 (2008).
  - [13] J. L. Sarrao *et al.*, Phys. Rev. B **59**, 6855 (1999).
  - [14] E. Bauer *et al.*, Physica B **234-236**, 676 (1997).
  - [15] T. Koyama *et al.*, Phys. Rev. B **66**, 014420 (2002).
  - [16] M. Ohtani *et al.*, unpublished.
  - [17] A. Yamamoto *et al.*, Physica B **403**, 1205 (2008).
  - [18] L. M. Falicov *et al.*, Phys. Rev. Lett. **22** 997 (1969).
  - [19] C. M. Varma, Rev. Mod. Phys. **48**, 219 (1976).
  - [20] W. E. Pickett *et al.*, Phys. Rev. B **23**, 1266 (1981).
  - [21] K. Takegahara *et al.*, J. Phys. Soc. Jpn. **59**, 3299 (1990).
  - [22] K. Yoshikawa *et al.*, Phys. Rev. B **72**, 165106 (2005).
  - [23] J. K. Freericks *et al.*, Phys. Rev. B **58**, 322 (1998).
  - [24] A. V. Goltsev *et al.*, Phys. Rev. B **63**, 155109 (2001).
  - [25] Y. Onishi *et al.*, J. Phys. Soc. Jpn. **69**, 3955 (2000).
  - [26] Y. Saiga *et al.*, J. Phys. Soc. Jpn. **77**, 114710 (2008).

- [27] A. A. Abrikosov *et al.*, *Methods of Quantum Field Theory in Statistical Physics* (Courier Dover Publications, 1975).
- [28] K. Yamada *et al.*, Prog. Theor. Phys. **76**, 621 (1986).
- [29] S. Watanabe *et al.*, Phys. Rev. Lett. **100**, 236401 (2008).
- [30] Even when  $\bar{\chi}_{\text{charge}}$  is not negligible for  $\bar{\chi}_{\text{spin}}^{\parallel}$ ,  $\chi_{+-}^{\text{eff}}(\mathbf{0}, 0)$  is expected to be greatly enhanced at  $T_v$  as well as the critical points.
- [31] J. C. Lashley *et al.*, Phys. Rev. Lett. **97**, 235701 (2006).
- [32] K. Miyake *et al.*, Physica B **259-261**, 676 (1999).
- [33] In case that coefficient  $A$  is very small  $\sim \mathcal{O}(V_{\mathbf{k}_F}/|\varepsilon_f|)^2$ , the dynamical exponent  $z_d$  is considered to be observed as  $\infty$ . Hence, as  $T$  decreases, the crossover of  $z_d$  from  $\infty$  to 2 or 3 at  $T = 0$  K is expected to be observed. For discussion about  $z_d = \infty$ , see ref. [6].
- [34] S. Watanabe and K. Miyake, unpublished.
- [35] P. Gegenwart *et al.*, Phys. Rev. Lett. **94**, 076402 (2005).
- [36] Z. Hossain *et al.*, Phys. Rev. B **72**, 094411 (2005).
- [37] S. Nakatsuji *et al.*, Nature Physics **4**, 603 (2008).